

Experimental Study on the Pressure and Pulse Wave Propagation in Viscoelastic Vessel Tubes—Effects of Liquid Viscosity and Tube Stiffness

Yuki Ikenaga, Shohei Nishi, Yuka Komagata, Masashi Saito, Pierre-Yves Lagrée, Takaaki Asada, and Mami Matsukawa, *Member, IEEE*

Abstract—A pulse wave is the displacement wave which arises because of ejection of blood from the heart and reflection at vascular bed and distal point. The investigation of pressure waves leads to understanding the propagation characteristics of a pulse wave. To investigate the pulse wave behavior, an experimental study was performed using an artificial polymer tube and viscous liquid. A polyurethane tube and glycerin solution were used to simulate a blood vessel and blood, respectively. In the case of the 40 wt% glycerin solution, which corresponds to the viscosity of ordinary blood, the attenuation coefficient of a pressure wave in the tube decreased from 4.3 to 1.6 dB/m because of the tube stiffness (Young's modulus: 60 to 200 kPa). When the viscosity of liquid increased from approximately 4 to 10 mPa·s (the range of human blood viscosity) in the stiff tube, the attenuation coefficient of the pressure wave changed from 1.6 to 3.2 dB/m. The hardening of the blood vessel caused by aging and the increase of blood viscosity caused by illness possibly have opposite effects on the intravascular pressure wave. The effect of the viscosity of a liquid on the amplitude of a pressure wave was then considered using a phantom simulating human blood vessels. As a result, in the typical range of blood viscosity, the amplitude ratio of the waves obtained by the experiments with water and glycerin solution became 1:0.83. In comparison with clinical data, this value is much smaller than that seen from blood vessel hardening. Thus, it can be concluded that the blood viscosity seldom affects the attenuation of a pulse wave.

I. INTRODUCTION

THE increase of mortality from cardiovascular disease (CVD), such as cardiac infarction and cerebral infarction, is a problem in developed countries. Because there are no subjective symptoms before development of these diseases, the medical treatment is often reactionary rather than preventative. The main cause of CVD is arteriosclerosis; its early detection is very important [1]–[5]. Arteriosclerosis is an excessive increase in aortic stiffness

as a result of aging or illness. It causes arterial stenosis and modifies the blood flow to tissues, resulting in the development of various disorders. Currently, there are several *in vivo* techniques to evaluate stiffness, such as the pulse wave velocity (PWV) method, cardio-ankle vascular index (CAVI), and ultrasonography, to evaluate arteriosclerosis [6]–[9]. Ultrasonography can be used for highly precise diagnoses and is suitable for diagnosing a structural abnormality that has already developed, such as stenosis. However, for the early detection of arteriosclerosis, it has become important to develop an *in vivo* technique to assess the initial hardening of the blood vessel in the early stages of arteriosclerosis [1]. Recently, the analysis of the pulse wave caused by intravascular pressure has attracted attention as a novel means of diagnosing arterial stiffness. Murgo *et al.* have reported that the wave profile also clearly changes with increasing arterial stiffness [10], [11]. In this situation, we have attempted to develop a new diagnostic method using a pulse wave. The pulse wave is a displacement wave of the skin surface that contains two displacement components, an incident wave, $\varepsilon_i(t)$, and a reflected wave, $\varepsilon_r(t)$. The reflected wave propagates a longer distance than the incident wave propagates, and contains the vessel stiffness information [1]. Therefore, the analysis of this wave is useful for the evaluation of vessel stiffness. Our group has reported a noninvasive method for extracting the reflected component from a pulse wave [12]–[14]. In this method, we first measured the pulse wave and the flow velocity at the left common carotid artery. We used a customized piezoelectric transducer which was developed by our laboratory in cooperation with Murata Manufacturing Co. Ltd. The resonant frequency of the sensor was about 40 kHz. At very low frequencies, the transducer measures the displacement. A transform of the conservation of mass, an elastic tube model, and a Voigt model for a viscoelastic body were used to estimate the displacement wave $\varepsilon_i(t) - \varepsilon_r(t)$ for the measured blood flow. Twice the amplitude of the reflected wave $2\varepsilon_r(t)$ (TARW) was obtained by subtracting the amplitude of the estimated displacement wave from that of the observed pulse wave. This method was applied to subjects of ages ranging from their twenties to sixties to evaluate differences in the reflected component. In the study, we also show that a one-dimensional model can simulate the wave propagation in a human body [15], [16]. In our former study, the

Manuscript received February 20, 2013; accepted July 15, 2013. Part of this work was supported by the Regional Innovation Strategy Support Program of the Ministry of Education, Culture, Sports, Science, and Technology.

Y. Ikenaga, S. Nishi, Y. Komagata, and M. Matsukawa are with the Faculty of Science and Engineering, Doshisha University, Kyoto, Japan (e-mail: mmatsuka@mail.doshisha.ac.jp).

M. Saito and T. Asada are with Murata Manufacturing Co. Ltd., Kyoto, Japan.

P.-Y. Lagrée is with CNRS and Université Pierre et Marie Curie Paris 6, Institut Jean le Rond d'Alembert, Paris, France.

DOI <http://dx.doi.org/10.1109/TUFFC.2013.2834>

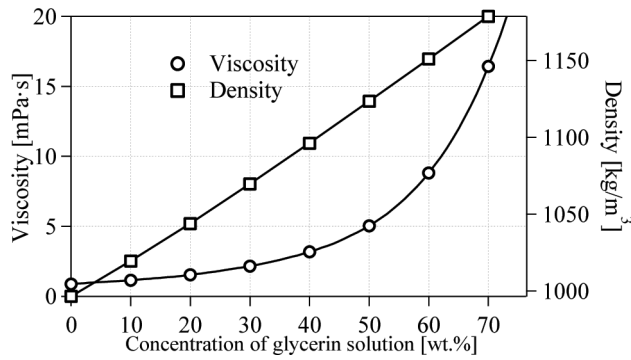


Fig. 1. Relationship between concentration of glycerin solution and liquid viscosity or density at 25°C [5].

relationship between age and the maximum value of the reflected wave showed moderate correlation between age and the amplitude of the reflected wave ($R^2 = 0.65$) [12]. To evaluate the validity of this method for screening arterial stiffness, TARW was compared with PWV and CAVI. TARW was moderately correlated with PWV ($R^2 = 0.48$) and CAVI ($R^2 = 0.71$) [12]. However, some dispersion was observed in the measurement results. If other factors that affect the amplitude of the reflected wave are found, we can obtain the modified amplitude of the reflected wave, which is a more highly precise index of vessel stiffness. It should be noted that as blood vessels stiffen, the attenuation of the reflected wave decreases [12]. On the contrary, if blood viscosity increases, attenuation is expected to increase. Blood viscosity then might affect the amplitude of the reflected wave. In this study, we focused on how the change of viscosity affects the reflected wave using an artery phantom. We experimentally investigated the effects of both blood viscosity and tube stiffness on the pressure wave propagation. A self-produced viscoelastic tube simulant of blood vessels and a pump which works as a heart reproducing a pulse flow were used. This paper is organized as follows: In Section II, a measurement system and materials used in the experiment are explained. Section III discusses the pressure wave propagation in viscoelastic tubes. The effects of the hardness of the tube and liquid viscosity on a pressure wave are investigated. In Sections IV and V, the validity of the experiment is evaluated by performing a numerical simulation using the one-dimensional model. The attenuation coefficients of the pressure wave are then estimated. Section VI explains the effect of blood viscosity on the pulse wave propagation. From an experiment using a phantom simulating a human blood vessel, the effect of blood viscosity on the attenuation of the pulse wave is also considered.

II. EXPERIMENT

A. Creating Viscoelastic Tubes

Two kinds of tubes (A and B) with different Young's moduli were fabricated using a polyurethane gel (Asker-C

5 and 15, Exseal Corp., Gifu, Japan). The diameter and thickness were set to 8 mm and 2 mm, respectively. The Young's modulus of tube A was approximately 200 kPa according to a tensile test (Ez-test, Shimadzu Corp., Kyoto, Japan); the Young's modulus of tube B was 60 kPa. The Young's modulus of an aged aorta ranges from 60 to 140 kPa [1]. The 200 kPa value for tube A is high; however, the blood vessels are not uniform and the Young's moduli are comparatively high in the distal part of the body [1]. Thus, the Young's moduli of tube A and tube B are considered to be appropriate examples for hard and soft blood vessels, respectively.

B. Creating Glycerin Solutions

Glycerin solutions were used in this experiment as a blood simulant. Taking the experimental temperature (room temperature 25°C) into consideration, glycerin solutions of 10, 20, 30, and 40 wt% were used. Fig. 1 shows the density and viscosity of this solution [17]. The viscosity of human blood is approximately 4 mPa·s [18], which is almost equivalent to the viscosity of a 40 wt% glycerin solution.

C. Measurement System and Procedure

The experimental system for the pressure wave is shown in Fig. 2. From a piston pump (custom-made, Tomita Engineering Co. Ltd., Osaka, Japan) that imitated the beating heart, the liquid was discharged to the tube that was filled with the same liquid. The end of the tube was occluded using a stainless-steel rod to prevent leakage. The liquids used were water and four kinds of glycerin solution. The length of tube A was 196.2 cm; the length of tube B was 180.1 cm. The lengths of the tubes were set so that the first wave and the second wave (reflected wave from the tube end) in Fig. 3 did not overlap. The input flow velocity waveform was a half-cycle sinusoidal wave. The period was 0.3 s and the total flow volume was 4.5 cm³. The pressure in the tube was measured using a pressure sensor (AP-10S, Keyence Corp., Osaka, Japan). The distances between the input and measurement points were 25.0 cm (point 1), 52.0 cm (point 2), and 82.6 cm (point 3).

III. EXPERIMENTAL RESULTS AND DISCUSSION

First, the observed pressure waveforms (liquid: water) are shown in Fig. 3. The first wave enclosed with the dashed line is a direct wave from the pump. The second wave is an overlapped wave of the reflection wave from the tube end and the re-reflected wave at the pump. Because the distance between the measurement point and pump is small, the reflected wave and the re-reflected wave are mostly overlapped. At measurement point 3, which is far from the pump, two peaks are seen in the second wave. The velocities of the pressure waves in tube A and tube

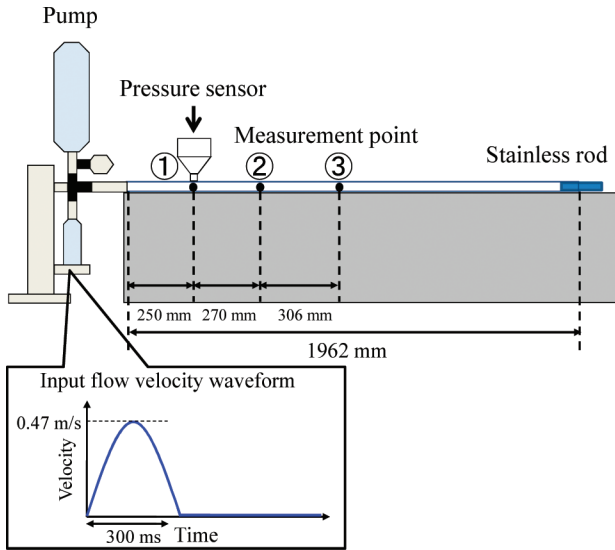


Fig. 2. Measurement system.

B are approximately 10 and 7 m/s. The amplitude of the first wave decreased as a result of the position, showing attenuation of the propagation. The same phenomenon occurred when using the glycerin solutions.

The pressure wave at point 1 is shown in Fig. 4. The amplitude of the first wave increased slightly, and the amplitude of a second wave decreased with increasing concentration of the glycerin solutions. In addition, the arrival time of the second wave changed because of the viscosity. The increase of viscosity is likely the reason. When the liquid viscosity and density increase, the impedance of the fluid increases and the amplitude of the first wave increases. In these liquids, the difference in the density is very small compared with the difference in the viscosity. Therefore, the amplitude of the first wave seems to increase as the viscosity increases. In addition, when the viscosity increases, the propagation loss increases and the amplitude of the second wave decreases. In each result, the offset of the waveform gradually increased over time. The black dashed line shows the offset in Figs. 3 and 4. This is because of the static pressure, which increased because of the liquid discharge and the inserted stainless rod.

IV. NUMERICAL CALCULATION

Next, a numerical calculation of the pressure wave propagation in the viscoelastic tube was performed using the one-dimensional model [15], [16], [19]. Our group has already reported the validity of this one-dimensional model for pulse wave propagation and applied it to a human artery model [15], [16], [19]. The following governing equations were used:

$$\frac{\partial A}{\partial t} + \frac{\partial Q}{\partial x} = 0 \quad (1)$$

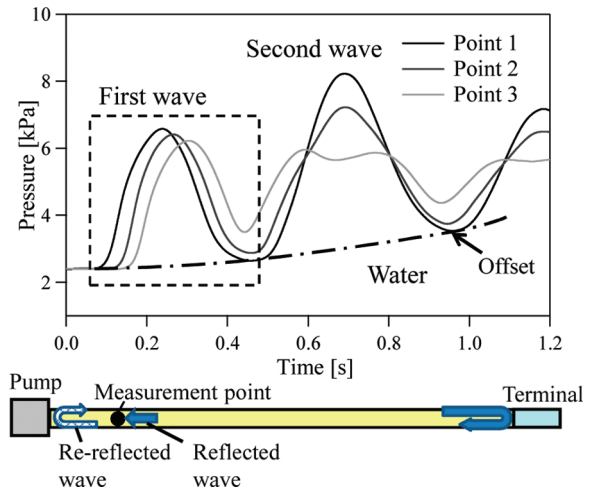


Fig. 3. Observed pressure waves at measurement points 1, 2 and 3 (water).

$$\frac{\partial Q}{\partial t} + \frac{4}{3} \frac{\partial}{\partial x} \left(\frac{Q^2}{A} \right) = -\frac{A}{\rho} \frac{\partial P}{\partial x} - \frac{8\nu Q}{R^2} \quad (2)$$

$$P = K((R - R_0) + \varepsilon_p(R - R_0)^2) + \eta \frac{\partial R}{\partial t}, \quad K = \frac{Eh}{(1 - \sigma^2)R^2}. \quad (3)$$

Each parameter is shown in Table I. Eq. (1) indicates conservation of mass, (2) is the momentum equation, and (3) indicates that the pressure perturbation is low. Because we cannot obtain the actual input pressure wave, the first wave at point 1 (Fig. 3) was used as the input waveform for the calculation. The experimental results and numerical computation are compared in Fig. 5. Here, the viscosity, density, and kinematic viscosity of water were used in the numerical calculation. The experimental result is a pressure wave at point 1. Because we used the observed first wave as the input for the calculation, the first waves are slightly different because of attenuation from the input point to point 1. The propagation velocity of a pressure wave depends on the Young's modulus of the tube. Thus,

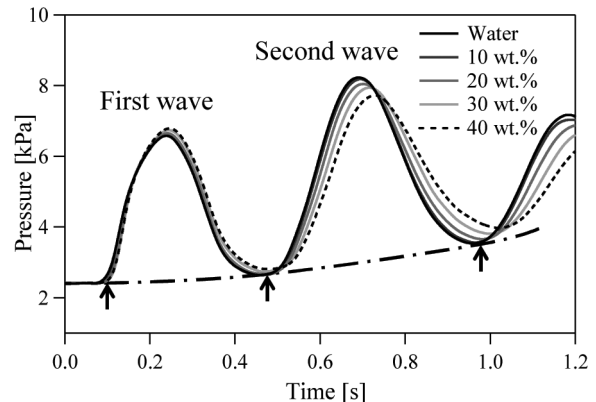


Fig. 4. Observed pressure waves by changing the liquids.

TABLE I. PARAMETERS IN THE 1-D THEORETICAL MODEL.

A	Tube's cross section	P	Intravascular pressure
R	Tube's radius	x	Longitudinal variable
R_0	Tube's initial radius (4 mm)	σ	Poisson's ratio (0.5)
K	Tube's bulk modulus	Q	Flux
η	Tube's viscosity	ρ	Fluid density
E	Tube's Young's modulus (173 kPa)	ν	Kinematic viscosity
h	Tube's thickness (2 mm)	ε_p	Nonlinear coefficient

we tuned the Young's modulus of the tube in the simulation. At this time, to estimate the best-matching theoretical waves, the cost functions were used. As can be seen, the numerical results are in good agreement with the experiments when the modulus was assumed to be 172 kPa. In addition, the optimum parameters were estimated as $\varepsilon_p = 0.052$, and $\eta = 0.038$. The 172 kPa was a little lower than the Young's modulus obtained by the tensile test. One reason may be the difference between static and dynamic measurements.

The numerical calculation was subsequently performed using a Young's modulus of 172 kPa. The results for the cases of glycerin solutions are shown in Fig. 6. The tendency of the pressure wave was similar to that of the experimental results shown in Fig. 4. The amplitude of the first wave increased and the amplitude of the second wave decreased because of the increase in viscosity of the liquid.

V. ATTENUATION COEFFICIENTS OF PRESSURE WAVES

We then estimated the attenuation coefficients of the pressure wave. The following processes were performed:

- 1) The change in static pressure resulting from the discharge of liquid was removed. Here, the change in static pressure was presumed at the minimum point of each wave in Fig. 4. The arrow (\uparrow) indicates the minimum point in the water case.
- 2) The reflection wave from the tube end and the re-reflected wave at the pump overlapped in the second wave. Here, the wavelength is very long and the arrival time difference of the overlapped waves is small.

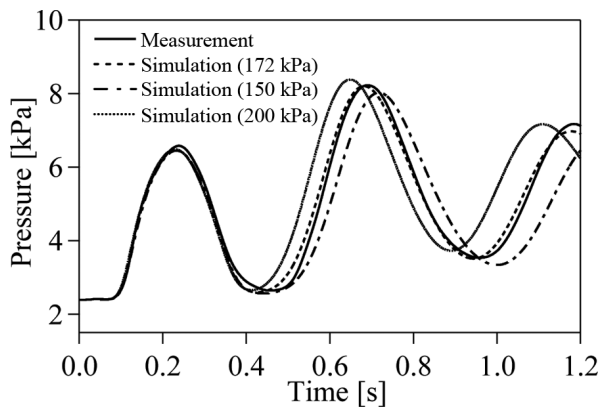


Fig. 5. Comparison between measurement and simulation for tube A.

Then, to estimate each amplitude, the amplitude of the second wave was subsequently divided in half.

The ratio of the amplitude spectra obtained from the first and second waves is shown in Fig. 7. Because the discharge period of the pump was 0.3 s, the fundamental frequency of the pulse was set to 1.67 Hz, and the attenuation coefficients at this frequency were estimated. The same processing was performed for the pressure wave acquired by numerical calculation, and the result is shown in Fig. 8. The experimental and calculated values showed good agreement. In this experiment, a solution with the glycerin concentration greater than 40 wt% was not used because of the limitations of the pump. However, the viscosity of human blood often increases to approximately 10 mPa·s when the hematocrit increases [18]. This viscosity is equivalent to a glycerin concentration of 60 wt%. To assess cases of high viscosities, complementary numerical calculations were performed. Fig. 8 shows an exponential increase of attenuation coefficients resulting from the change in concentration of the glycerin solution. The results for tube B are also shown in Fig. 8. In the case of a glycerin solution of 40 wt% (normal blood viscosity), the attenuation coefficient changed from 1.6 to 4.3 dB/m because of the tube stiffness. This means that as the tube softens, the attenuation coefficient increases when the tube becomes softer, indicating that the amplitude of the reflected wave decreases. In the range of human blood [18], in tube A, the attenuation coefficients of a pressure wave changed from 1.6 to 3.2 dB/m as the viscosity of the liquid increased. Therefore, liquids with high viscosities decrease the amplitude of the reflected wave. The hardening of blood vessels by aging or illness, and the increase of

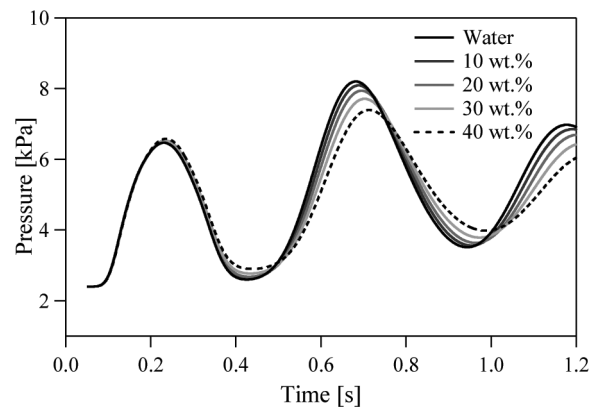


Fig. 6. Calculated pressure waves by changing the liquids for tube A.

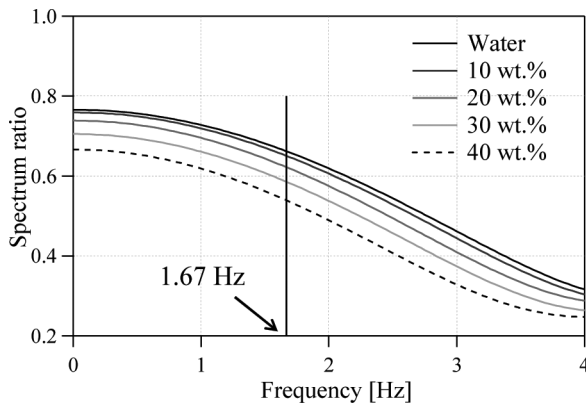


Fig. 7. Spectrum ratio of first and second waves for tube A.

blood viscosity have opposite effects on the intravascular pressure wave. These opposite effects may occur in human arteries and be one reason for the dispersion of the reflected wave amplitude *in vivo* [12].

VI. HUMAN ARTERY PHANTOM

A simple human artery phantom was also created to consider the effect of blood viscosity on the amplitude of the reflected wave. Water or a glycerin solution was ejected into the phantom and the amplitude of the reflected wave measured by the *in vivo* technique [12]–[14] was considered.

A. Details of the Model

A simple human artery phantom consisting of a main artery, a left carotid artery, a femoral artery, and a subclavian-radial artery on right and left sides was designed. The phantom was made of polyurethane, with a Young's modulus of approximately 200 kPa [tensile test], which was the same as that of tube A. The details of the model are shown in Fig. 9 and Table II. The length of each blood vessel was defined based on vessel data of an average adult man [20]. The diameter and thickness were determined so that the reflection coefficient at a bifurcation was negli-

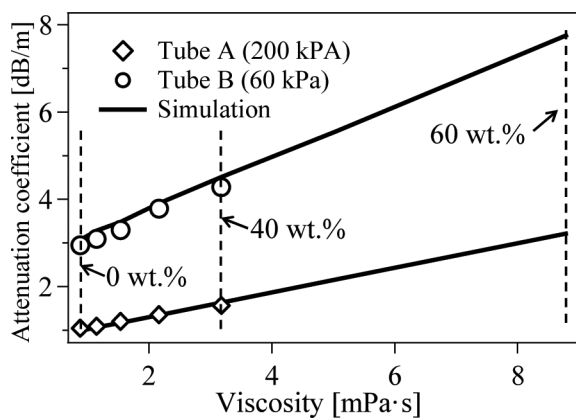


Fig. 8. Attenuation coefficients obtained from spectrum ratio.

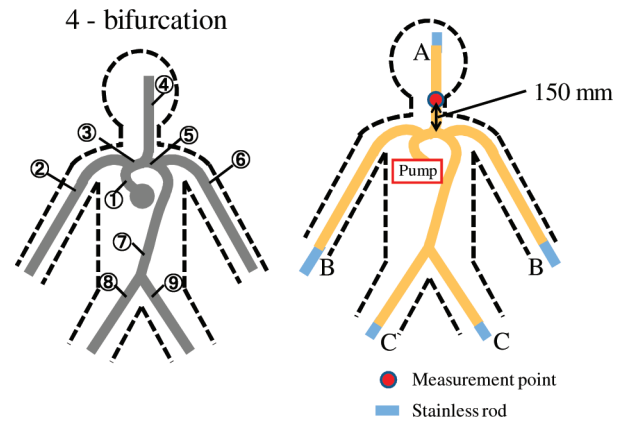


Fig. 9. Measurement system of human artery phantom with four bifurcations.

ble. In addition, the end of each tube was regarded as the vascular bed at the peripheral site, which is considered to be a reflecting point of the pulse wave in the human body. The reflection coefficient at this site is approximately 0.8 [1]. However, in the experiment, the tube end was closed (reflection coefficient: 1.0), because it was difficult to reproduce the reflection coefficient of 0.8.

B. Measurement System and Procedure

The experimental system is shown in Fig. 9. From a custom-made piston pump (Tomita Engineering Co. Ltd.) that simulated the heart, the liquid was discharged to the model, which was filled with the same liquid. The tube ends were occluded using a stainless-steel rod to prevent leakage. The liquids used were water or 40 wt% glycerin solution. The flow velocity waveform was a half-cycle sinusoidal wave. The period was 0.3 s and the total flow volume was 4.5 cm³. The measurement point was set at 150 mm from the second bifurcation to point A. This point was assumed as the carotid artery of the neck in an actual human body. In our previous paper, this point corresponds to the measurement point in the *in vivo* system [12]–[14]. We measured the inner pressure wave and flow velocity in the human artery model. We used a pressure sensor (AP-10S, Keyence Corp.) to measure the inner pressure wave and an ultrasonic Doppler system (Aplio SSA-700A, Toshiba Medical Systems Corp., Tokyo, Japan) to measure the flow velocity. The center frequency of the ultrasonic pulse (probe PLT-1204AT, Toshiba Medical Systems Corp.) was 12 MHz.

C. Measurement Results and Discussion

The observed pressure wave and the flow velocity waveform are shown in Figs. 10 and 11. The pressure wave includes various reflected waves. The first point at which the slope of the pressure wave becomes gentle was defined as the maximum amplitude of the direct incident wave (incident peak). In each waveform, the amplitude was normalized with the incident peak. The reflected wave was

TABLE II. DETAILS OF A SIMPLE HUMAN ARTERY MODEL.

	Name	Length (mm)	Diameter (mm)	Thickness (mm)
1	Aorta arch A	35	12	2
2	R subclavian radial artery	800	6	1.5
3	Aorta arch B	28	11	2
4	L carotid artery	650	6	1.5
5	Aorta arch C	42	10	2
6	L subclavian radial artery	72.7	6	1.5
7	Aorta	460	8	1.5
8	R femoral artery	318	6	1.5
9	L femoral artery	327	6	1.5

Numbers in the first column correspond to circled numbers in Fig. 9.

extracted from these two waves using the technique for *in vivo* measurement [10]. The procedure of the *in vivo* technique is shown in Fig. 12. Here, the input flow velocity and pressure wave are defined as $u_1(t)$ and $P_1(t)$. The reflected flow velocity and pressure wave from point A and points B and C are defined as $u_{ra}(t)$, $P_{ra}(t)$, $u_{rbc}(t)$ and $P_{rbc}(t)$, respectively. We estimated the pressure wave [$P_1(t) - P_{ra}(t) + P_{rbc}(t)$] from the measured flow wave [$u_1(t) - u_{ra}(t) + u_{rbc}(t)$]. In step 2, to estimate the apparent pressure wave, a transform of the conservation of mass and an elastic tube model were used. The reflected wave was subsequently extracted by subtracting the estimated pressure wave from the measured pressure wave [$p_1(t) + p_{ra}(t) + p_{rbc}(t)$]. The flow velocity wave contained a virtual negative reflection that originated from point A. The amplitude of the extracted reflected wave from point A [$2p_{ra}(t)$] was then doubled. Therefore, the reflected wave was divided in half [$p_{ra}(t)$]. On the other hand, the pressure wave with positive amplitude was estimated from the reflected flow waves generated at points B and C. In this case, the observed and estimated reflected waves [$p_1(t)$ and $p_{rbc}(t)$] canceled each other. Therefore, the first peak of the estimated reflected wave is the wave reflected at point A. The obtained reflected waves are shown in Fig. 13. Because one end of the tube is closed, it is possible that the static pressure increased.

The relationship between the attenuation coefficient of the pressure wave and the amplitude of reflected waves was then considered. The ratio of P_1 and P_2 of the experimental result was 1: 0.92. According to Fig. 8, the dif-

ferences of the attenuation coefficient between water and glycerin 40 wt% (viscosity; 3.2 mPa·s) was 0.6 dB/m. The reflected wave made a round trip between the measurement point and the reflecting point A; the propagation distance was approximately 1 m. The attenuation then corresponds to the ratio of P_1 to P_2 of 1:0.93. There is good agreement between both results. If the hematocrit value increases, the blood viscosity increases by 2 to 3 times [14]. According to Fig. 8, in this blood viscosity range, the attenuation coefficient changes by 1.6 dB/m. The amplitude ratio then becomes 1:0.83. According to the results shown in Fig. 1, the amplitude ratio becomes 0.36:0.30. The effect of attenuation in people in their twenties is shown in Fig. 14. Thus, it can be concluded that the viscosity of blood weakly affects the attenuation of a pulse wave.

VII. CONCLUSION

In this study, we experimentally investigated the effects of both blood viscosity and tube stiffness on the pressure wave propagation using artificially fabricated tubes. Viscoelastic tubes A (200 kPa) and B (60 kPa) were used to simulate blood vessels. Glycerin solutions less than 9 mPa·s were used as blood simulants for the normal situation. The pressure wave propagation in the tube was measured, and the attenuation coefficient was calculated.

In the case of glycerin solution of 40 wt%, which corresponds to ordinary blood viscosity, the attenuation coef-

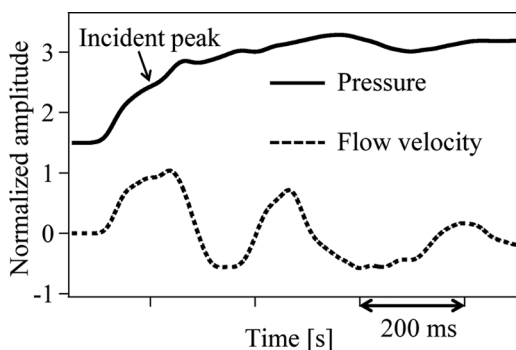


Fig. 10. Observed pressure wave and flow velocity waveform (water) in the phantom.

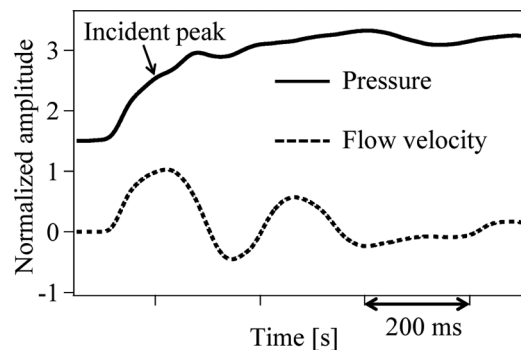


Fig. 11. Observed pressure wave and flow velocity waveform (glycerin 40 wt%) in the phantom.

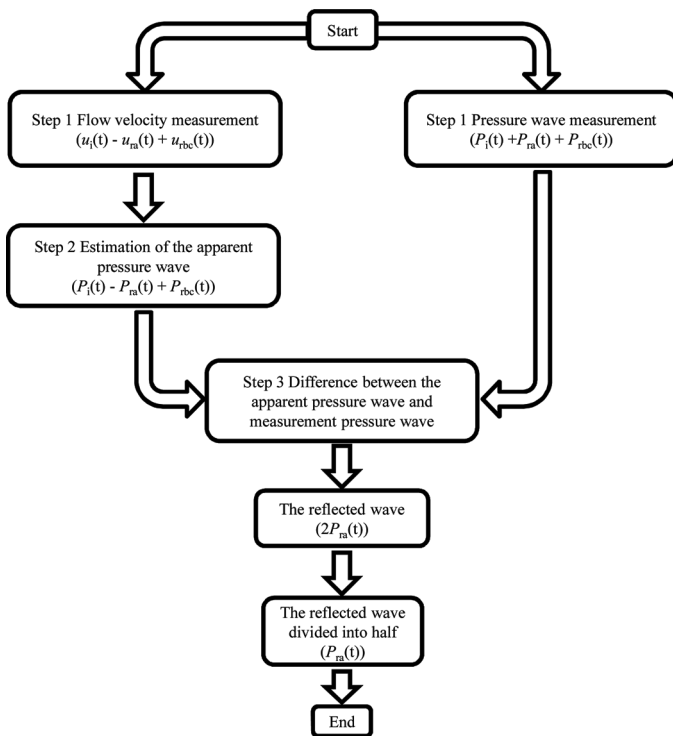


Fig. 12. The procedure for the extraction of reflected waves.

ficient of a pressure wave changed from 1.6 to 4.3 dB/m because of the tube stiffness. In the range of human blood viscosity, the attenuation coefficient of a pressure wave changed from 1.6 to 3.2 dB/m because of the viscosity. The hardening of blood vessels by aging and the increase of blood viscosity seem to have opposite effects on intravascular pressure waves. However, from the results of an experiment using a human artery model, the effect of blood viscosity on the attenuation of a pressure wave seemed negligible. The human arterial network has a complicated structure, and the propagation characteristics of the pressure waves and pulse waves through this network are not yet solved in detail. The flow measurement also seems to contain some errors during *in vivo* measurements. For clarification of the pulse wave characteristics, especially the reflected wave component, further study is necessary through both experiments and numerical calculation.

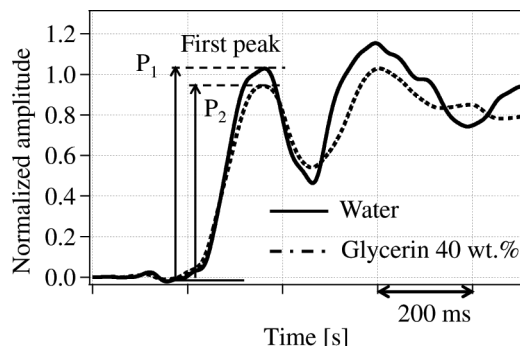


Fig. 13. Comparison of the reflected wave obtained by the experiment.

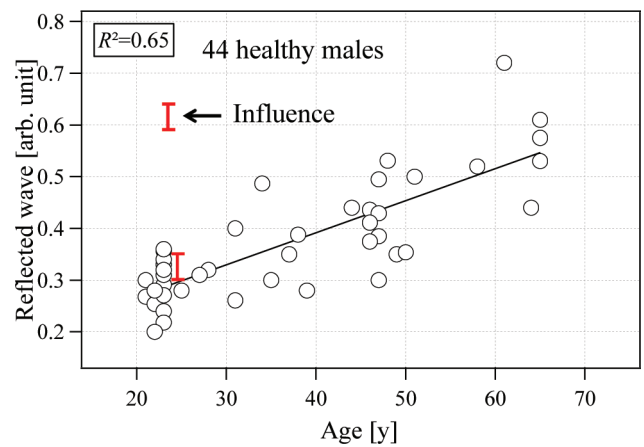


Fig. 14. Relationship between age and maximum value of the reflected wave [4].

REFERENCES

- [1] W. W. Nichols and M. F. O'Rourke, *McDonald's Blood Flow in Arteries*, 5th ed., London, UK: HodderArnold, 2005.
- [2] G. F. Mitchell, H. Parise, E. J. Benjamin, M. G. Larson, M. J. Keyes, J. A. Vita, R. S. Vasan, and D. Levy, "Changes in arterial stiffness and wave reflection with advancing age in healthy men and women," *Hypertension*, vol. 43, no. 6, pp. 1239–1245, 2004.
- [3] I. E. Kallikazaros, C. P. Tsioufis, C. I. Stefanadis, C. E. Pitsavos, and P. K. Toutouzas, "Closed relation between carotid and ascending aortic atherosclerosis in cardiac patients," *Circulation*, vol. 102, no. 19, suppl. 3, pp. III-263–III-268, 2000.
- [4] H. Hasegawa and H. Kanai, "Modification of the phased-tracking method for reduction of artifacts in estimated artery wall deformation," *IEEE Trans. Ultrason. Ferroelectr. Freq. Control*, vol. 53, no. 11, pp. 2050–2064, 2006.
- [5] H. M. Loree, A. J. Grodzinsky, S. Y. Park, L. J. Gibson, and R. T. Lee, "Static circumferential tangential modulus of human atherosclerotic tissue," *J. Biomech.*, vol. 27, no. 2, pp. 195–204, 1994.
- [6] P. Avolio, S. G. Chen, R. P. Wang, C. L. Zhang, M. F. Li, and M. F. O'Rourke, "Effects of aging on changing arterial compliance and left ventricular load in a northern Chinese urban community," *Circulation*, vol. 68, no. 1, pp. 50–58, 1983.
- [7] A. Takaki, H. Ogawa, T. Wakeyama, T. Iwami, M. Kimura, Y. Hadano, S. Matsuda, Y. Miyazaki, T. Matsuda, A. Hiratsuka, and M. Matsuzaki, "Cardio-ankle vascular index is a new noninvasive parameter of arterial stiffness," *Circ. J.*, vol. 71, no. 11, pp. 1710–1714, 2007.
- [8] P. H. Davis, J. D. Dawson, L. T. Mahoney, and R. M. Lauer, "Increased carotid intimal-medial thickness and coronary calcification are related in young and middle-aged adults," *Circulation*, vol. 100, no. 8, pp. 838–842, 1999.
- [9] K. Cruickshank, L. Riste, S. G. Anderson, J. S. Wright, G. Dunn, and R. G. Gosling, "Aortic pulse-wave velocity and its relationship to mortality in diabetes and glucose intolerance: An integrated index of vascular function?" *Circulation*, vol. 106, no. 16, pp. 2085–2090, 2002.
- [10] J. P. Murgu, N. Westerhof, J. P. Giolma, and S. A. Altobelli, "Aortic input impedance in normal man: Relationship to pressure wave forms," *Circulation*, vol. 62, no. 1, pp. 105–116, 1980.
- [11] J. P. Murgu, N. Westerhof, J. P. Giolma, and S. A. Altobelli, "Manipulation of ascending aortic pressure and flow wave reflections with the Valsalva maneuver: Relationship to input impedance," *Circulation*, vol. 63, no. 1, pp. 122–132, 1981.
- [12] M. Saito, M. Matsukawa, T. Asada, and Y. Watanabe, "Noninvasive assessment of arterial stiffness by pulse wave analysis," *IEEE Trans. Ultrason. Ferroelectr. Freq. Control*, vol. 59, no. 11, pp. 2411–2419, 2012.
- [13] M. Saito, Y. Yamamoto, M. Matsukawa, Y. Watanabe, M. Furuya, and T. Asada, "Simple and noninvasive analysis of the pulse wave for blood vessel evaluation," in *IEEE Int. Ultrasonics Symp. Proc.*, 2009, pp. 1934–1937.

- [14] M. Saito, Y. Yamamoto, Y. Shibayama, M. Matsukawa, Y. Watanabe, M. Furuya, and T. Asada, "Estimation of reflected wave in carotid pulse wave for simple and noninvasive assessment of arterial stiffness," in *IEEE Int. Ultrasonics Symp. Proc.*, 2010, pp. 1934–1937.
- [15] M. Saito, Y. Ikenaga, M. Matsukawa, Y. Watanabe, T. Asada, and P.-Y. Lagr e, "One-dimensional model for propagation of a pressure wave in a model of the human arterial network: Comparison of theoretical and experimental results," *J. Biomech. Eng.*, vol. 133, no. 12, art. no. 121005, 2011.
- [16] M. Saito, Y. Ikenaga, M. Matsukawa, Y. Watanabe, T. Asada, and P.-Y. Lagr e, "1D model for propagation of pulse wave in an arterial network: Comparative study of theory and experiment," in *2011 IEEE Int. Ultrasonics Symp. Proc.*, pp. 713–716.
- [17] The Japan Society of Mechanical Engineers, "Ryutai-no-netsubuseichi-shu (Thermophysical properties of fluids)," *JSME Data Book*, Tokyo, Japan: JSME, 1983, pp. 277–478 (In Japanese).
- [18] A. C. Guyton, *Textbook of Medical Physiology*, 8th ed., Philadelphia, PA: Saunders, 1991, p. 157.
- [19] X. Wang, O. Delestre, J.-M. Fullana, M. Saito, Y. Ikenaga, M. Matsukawa, and P.-Y. Lagr e, "Comparing different numerical methods for solving arterial 1D flows in networks," *Comput. Methods Biomech. Biomed. Engin.*, vol. 15, suppl. 1, pp. 61–62, 2012.
- [20] N. Westerhof, F. Bosman, C. J. De Vries, and A. Noordergraaf, "Analog studies of the human systemic arterial tree," *J. Biomech.*, vol. 2, no. 2, pp. 121–143, 1969.



Masashi Saito was born in Gunma, Japan, in December 1983. He received the Ph.D. degree in engineering from Doshisha University, Kyoto, Japan, in 2012. He is currently working as an engineer at Murata Manufacturing Co. Ltd., Kyoto, Japan. His research interests include ultrasonic electronics and biomechanical engineering.



Pierre-Yves Lagr e was born in Courri res, France, in 1965. He joined Ecole Normale Sup rieure Saint-Cloud/Lyon in 1985, and obtained the Agr gation de Physique in 1988. He stayed one year at ONERA. He received the Ph.D. degree in fluid mechanics in 1992 from University Paris 6. Currently, he is Senior Scientist in CNRS at the Institute Jean le Rond d'Alembert Paris 6, France. His research interests include biomechanics.



Takaaki Asada was born in Nara, Japan. He received the Dr.Eng. degree from Doshisha University, Kyoto, Japan, in 1992. He joined Murata Mfg. Co. Ltd. in 1992. Currently, he is a manager in the Product Development Department of the Sensor Products Division, Murata Mfg. Co. Ltd., Japan. He has also been a visiting professor in the Faculty of Science and Engineering, Doshisha University, since 2009. His interests include piezoelectric devices, impulsive acoustic sources, and their commercialization.



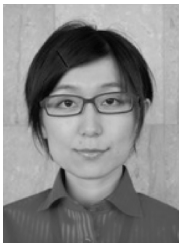
Yuki Ikenaga was born in Osaka, Japan, in November 1988. He received the master's degree in engineering from Doshisha University, Kyoto, Japan, in 2013. He is currently working as an engineer at Nissan Motor Co. Ltd., Kanagawa, Japan. His research interests include ultrasonic electronics and viscoelastic bodies.



Shohei Nishi was born in Osaka, Japan, in December 1990. He received the bachelor's degree in engineering from Doshisha University, Kyoto, Japan, in 2013. He is majoring in electrical engineering at Doshisha University. His research interests include ultrasonic electronics and vascular vessel systems.



Mami Matsukawa was born in Kyoto, Japan. She joined the National Institute of Advanced Industrial Science and Technology (AIST), Ministry of International Trade and Industry (MITI), in Osaka, Japan. She received the Dr.Eng. degree from Doshisha University, Kyoto, Japan, in 1993. Currently, she is a professor in the Faculty of Science and Engineering, Doshisha University, Japan. Her research interests include bone quantitative ultrasound, Brillouin scattering, pulse waves, and ultrasonic electronics. She is a member of IEEE.



Yuka Komagata was born in Niigata, Japan, in 1988. She graduated from Doshisha University, Kyoto, Japan, in 2012. She is in the graduate school of Doshisha University, Kyoto, Japan. Her interests include ultrasonic electronics and biomedical engineering.